AD-A152 243 THERMOMECHANICAL CONTACT PHENOMENA AND WEAR OF FACE SEALS(U) THAYER SCHOOL OF ENGINEERING HANOVER N H F E KENNEDY ET AL. JAN 85 N00014-81-K-0090 8/8

UNCLASSIFIED F/G 11/1 NL

END
DATE FILMED
10-85

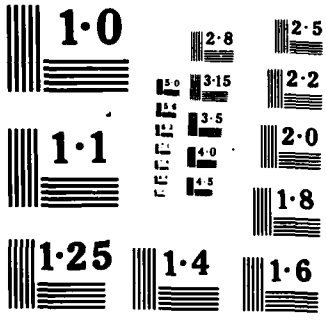
1·0
1·1
1·25
1·4
1·6
1·8
2·0
2·2
2·5
2·8
3·15
3·5
4·0
4·5

6

THERMOMECHANICAL CONTACT PHENOMENA AND WEAR OF FACE SEALS

by

Francis E. Kennedy, Jr.
Associate Professor of Engineering

and

Chong-Khai Chuah and Wilhelm Brote
Graduate Research Assistants

Annual Report #4

submitted to

Office of Naval Research
Contract No. N00014-81-K-0090
Period Covered: December 1, 1983 to November 30, 1984

January 1985

THAYER SCHOOL OF ENGINEERING
a professional school of Dartmouth College
Hanover, New Hampshire 03755

Unclassified
SECURITY CLASSIFICATION OF THIS PAGE

REPORT DOCUMENTATION PAGE

1a. REPORT SECURITY CLASSIFICATION Unclassified	1b. RESTRICTIVE MARKINGS
2a. SECURITY CLASSIFICATION AUTHORITY	3. DISTRIBUTION / AVAILABILITY OF REPORT Approved for public release; distribution unlimited
2b. DECLASSIFICATION / DOWNGRADING SCHEDULE	
4. PERFORMING ORGANIZATION REPORT NUMBER(S) Annual Report ONR #4	5. MONITORING ORGANIZATION REPORT NUMBER(S)
6a. NAME OF PERFORMING ORGANIZATION Dartmouth College 6b. OFFICE SYMBOL (*If applicable*)	7a. NAME OF MONITORING ORGANIZATION Office of Naval Research
6c. ADDRESS (*City, State, and ZIP Code*) Thayer School of Engineering Hanover, N.H. 03755	7b. ADDRESS (*City, State, and ZIP Code*) Engineering Science Directorate Arlington, Virginia 22217
8a. NAME OF FUNDING / SPONSORING ORGANIZATION Office of Naval Research 8b. OFFICE SYMBOL (*If applicable*)	9. PROCUREMENT INSTRUMENT IDENTIFICATION NUMBER N00014-81-K-0090
8c. ADDRESS (*City, State, and ZIP Code*) Engineering Science Directorate Arlington, Virginia 22217	10. SOURCE OF FUNDING NUMBERS PROGRAM ELEMENT NO. 61153N 24 / PROJECT NO. NR 091-044 / TASK NO. RR024-03-03 RMS 2403-032 / WORK UNIT ACCESSION NO
11. TITLE (*Include Security Classification*) Thermomechanical Contact Phenomena and Wear of Face Seals	
12. PERSONAL AUTHOR(S) Francis E. Kennedy, Jr. Chong-Khai Chuah, F.O. Wilhelm Brote	
13a. TYPE OF REPORT Annual Report 13b. TIME COVERED FROM 83/12/1 TO 84/11/30	14. DATE OF REPORT (*Year, Month, Day*) 1985 January 30 15. PAGE COUNT 41
16. SUPPLEMENTARY NOTATION	

17. COSATI CODES			18. SUBJECT TERMS (*Continue on reverse if necessary and identify by block number*)
FIELD	GROUP	SUB-GROUP	Mechanical Seals, Face Seals, Wear, Thermoelastic Instability
11	01		

19. ABSTRACT (*Continue on reverse if necessary and identify by block number*)

Contact between the two seal rings of a mechanical face seal was monitored using a unique contact probe. It was found that several discrete patches of solid-to-solid contact exist at the contact interface, whether the seal be run dry or with a sealed liquid. Seal profiles were determined using a computer-aided profilometry system before and after seal operation. Comparison between the surface profiles and the contact measurements showed that the contact patches occur at the waviness peaks on the harder and stiffer of the two rings. Wear occurs only within those patches and this results in increased surface roughness. The total wear of the seal rings was considerably greater for a material with larger patch sizes resulting, at lease in part, from increased thermal conductivity.

20. DISTRIBUTION / AVAILABILITY OF ABSTRACT ☒ UNCLASSIFIED/UNLIMITED ☐ SAME AS RPT. ☐ DTIC USERS	21. ABSTRACT SECURITY CLASSIFICATION Unclassified
22a. NAME OF RESPONSIBLE INDIVIDUAL A.W. Ruff	22b. TELEPHONE (*Include Area Code*) (202)696-4401 22c. OFFICE SYMBOL ONR Code 431

DD FORM 1473, 84 MAR 83 APR edition may be used until exhausted.
All other editions are obsolete.

SECURITY CLASSIFICATION OF THIS PAGE

THERMOMECHANICAL CONTACT PHENOMENA AND WEAR OF FACE SEALS

Annual Report #4

submitted to

Office of Naval Research
Contract No. N00014-81-K-0090
Period Covered: December 1, 1983 to November 30, 1984

by

Francis E. Kennedy, Jr.
Associate Professor of Engineering

and

Chong-Khai Chuah and Wilhelm Brote
Graduate Research Assistants

Thayer School of Engineering
Dartmouth College
Hanover, New Hampshire 03755

January 1985

FOREWORD

Work at the Thayer School of Engineering at Dartmouth College on this project has been supported by Office of Naval Research Contract No. N00014-81-K-0090. Dr. A. William Ruff has been the ONR contract monitor during the past year.

Mr. Victor A. Surprenant of Dartmouth College assisted in materials aspects of the research and both he and Sidney A. Karpe of the David Taylor Naval Ship R&D Center in Annapolis contributed measurably to discussions about the observed seal contact phenomena.

Carbon graphite seal rings for the experimental program were contributed by EG&G Sealol, Inc.

TABLE OF CONTENTS

LIST OF FIGURES

LIST OF TABLES

INTRODUCTION AND BACKGROUND

The sealing surfaces of mechanical face seals are generally lapped flat and parallel prior to operation. Despite this, non-uniform solid-to-solid contact can occur at the interface. Consequently, frictional tractions and frictional heating can vary around the seal ring circumference. Burton and others [1-3] have shown that the non-uniform heating may, by the process known as thermoelastic instability, lead to the concentration of contact into a small number of hot, highly stressed contact patches. These patches are much larger and fewer in number than the uniformly distributed asperity contacts normally assumed to comprise the contact interface. It has been shown that the large thermal stress near the hot contacts could be responsible for the thermocracks, or heat checks, that frequently are seen on seal rings after severe operation [4].

Proof of the existence of hot patches of solid-to-solid contact has been obtained experimentally in the case of metallic rings rotating against a non-metallic disk [3] and, more recently, in actual operating face seals [5]. The latter study made use of a new contact probe which enables the monitoring of contact patch sizes and locations in ring-on-ring or ring-on-disk configurations. It has proven quite effective in determining the geometry and movement of contact patches in dry operation of mechanical face seals [5]. When used in conjunction with numerical thermal and stress analyses, the probe allowed determination of distributions of frictional heat, contact pressure, and stress in the contact patch regions [6].

The earlier studies provided much information about contact patches in dry operation of face seals and the factors that affect them. For example, in dry operation of seals consisting of a carbon graphite ring in contact with a metallic ring, it was found [5] that solid/solid contact is concentrated in a few (2 to 5) patches which remained stationary with respect to the metallic

seal ring. The patch length was smaller, and surface temperatures higher, at higher seal velocities and with metallic rings having lower thermal conductivity or greater hardness [5,6]. These results agreed with earlier theoretical analyses of the phenomenon [1].

It was the purpose of this work to extend the previous experimental studies [5,6] in order to gain a better understanding of contact phenomena in face seals. Of particular interest were the following:

1. Extension of the experimental study of seal contact conditions to liquid lubricated seals. Previous attempts at using the contact probe with sealed liquids had met with failure, owing to the leakage of electrical current through the thin liquid film present between the seal faces [5].

2. A controlled study of the relationship between contact conditions and wear within the contact patches. It has been proven theoretically that wear can affect the thermoelastic instability that results in patch formation [7], but the inverse relationship, i.e., the effect of contact patch conditions on wear had not been studied.

3. Determination of the relationship between contact patch locations and the surface profile of the seal rings. Although it has been shown that thermoelastic instability can occur with flat contacting surfaces [1], it was hypothesized that the origin of the contact nonuniformities was the initial waviness of the seal faces. This work set out to prove that hypothesis.

METHODS AND MATERIALS

Apparatus and Test Procedures

The seals used in this program were slightly modified versions of a mechanical face seal designed for turbine engine applications. The seal has a carbon graphite primary ring, which in these tests served as the stationary

seal ring. The rotating ring was metallic.

The seal rings were mounted in specially designed holders. The holder with the rotating ring was mounted on the spindle of a modified drill press. The stationary specimen holder was mounted on a thrust bearing beneath the spindle and was surrounded by a test chamber which could serve to collect leakage from the seal. Rotation of the test chamber was limited by a torque-sensing system for friction determination. Normal load was applied through the spindle by a static weight hung on the loading arm. The spindle was rotated at a preset speed ranging from 15.7 rad/s to 188.5 rad/s (surface velocity of the rotating ring ranging from 0.41 to 4.95 m/s).

The stationary carbon seal ring had two very small (0.22 mm diameter) holes drilled in it, perpendicular to the contact surface. One of the holes was near the ring inside diameter and the other near the outside diameter. Fine wires (0.18 mm diameter) were mounted in each hole to act as contact probes [5]. The wires were bonded in the ring with an electrically insulating adhesive and the surface of the ring was then lapped and polished. The wires therefore formed part of the seal ring surface, but were electrically insulated from the rest of the ring. The probe wires were made from constantan so that they could also act as one leg of a dynamic thermocouple [5]. The other side of the contact probe circuit, and thus the other leg of the thermocouple, was the rotating metallic seal ring. Electrical connection was made to the rotating seal ring through a carbon electrical brush at the ring outside diameter. A schematic diagram of the test apparatus is shown in Figure 1.

To allow the possibility of liquid lubricated seal tests, a means was provided to supply pressurized fluid to the interior of the seal. For these tests the fluid was tap water and its pressure could be controlled by a regulator in the supply line (Figure 1). The flexible supply line tubing did not inhibit friction measurement.

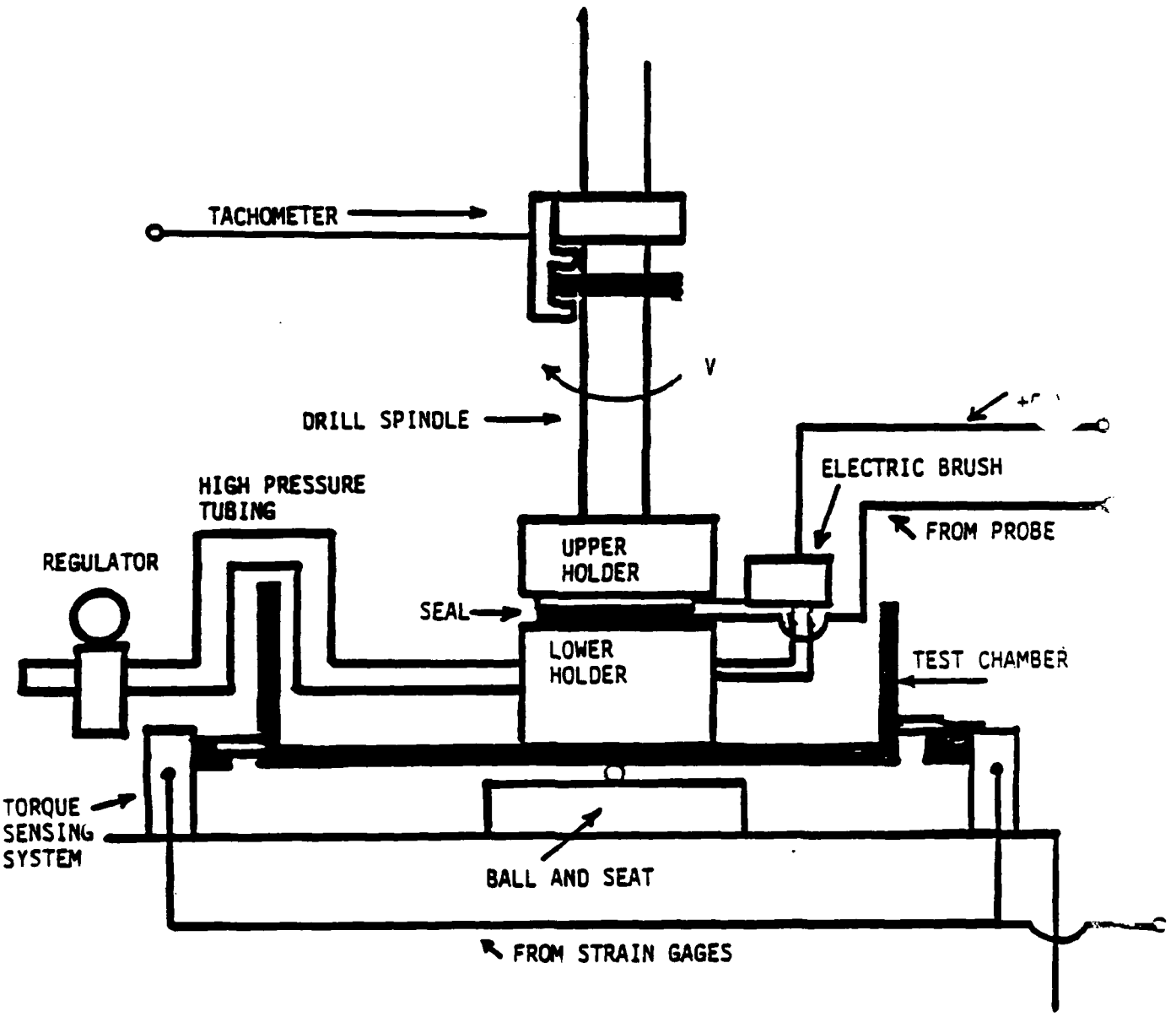

FIGURE 1. SCHEMATIC DIAGRAM OF TEST APPARATUS

During a test, the contact probe/thermocouple worked as follows [5]: In the probe mode, a 5 volt D.C. signal was applied to the rotating ring via the electrical brush. Both probe wires were monitored using an oscilloscope. If the wire location on the stationary ring was in intimate contact with the rotating ring, a 5 volt signal appeared on the scope; otherwise zero volts appeared. The oscilloscope trace was triggered at the same point on the rotating ring each revolution. Therefore, the probe output could be used to locate contact patches, determine their size (from the width of the 5 V pulses) and monitor their motion relative to the moving ring. In the thermocouple mode the 5 V input signal was turned off and, instead, the emf generated by the dynamic thermocouple junction was monitored, enabling temperatures of the contact patches to be approximated.

Wear of the seal rings was determined by weight loss measurements. Each of the seal rings was weighed on an accurate analytical balance before and after each test run.

Analysis of the surface profiles of the seal rings both before and after wear tests was performed using computerized profilometry equipment. The system was built around a linear profilometer which was modified to enable seal ring topography to be measured. A high accuracy, motor driven, air bearing rotary table was used to rotate the ring-shaped specimens beneath the profilometer's stationary stylus head. A fixture was built to accurately center and level the seal ring on the rotary table.

A more complete characterization of the surface topography was desired than that given by the analog output of the profilometer. A digital data acquisition system was used to acquire and digitize the surface profile data and to pass the data to a digital computer for data analysis. The analysis software accomplished the removal of ring tilt from the topography

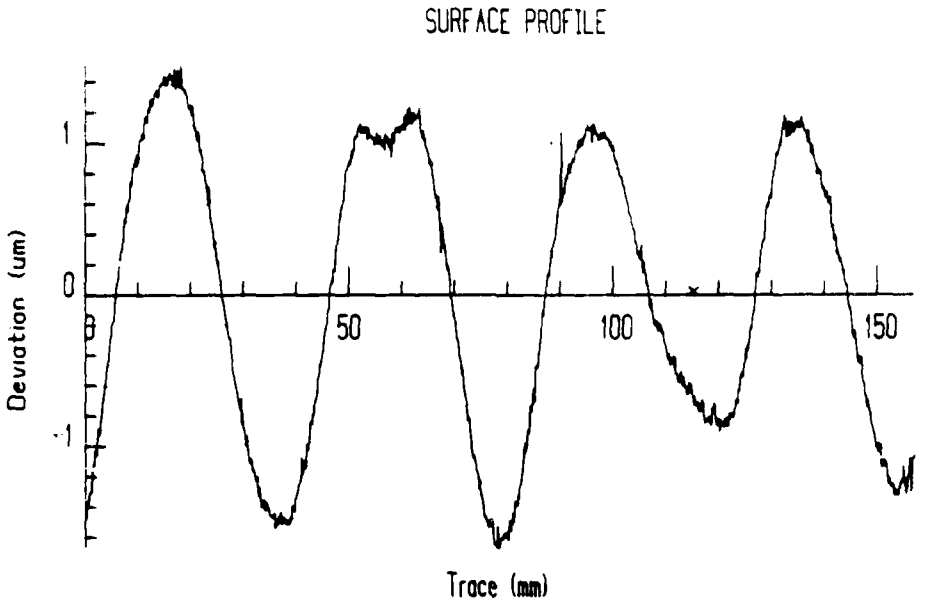

(a) Before test

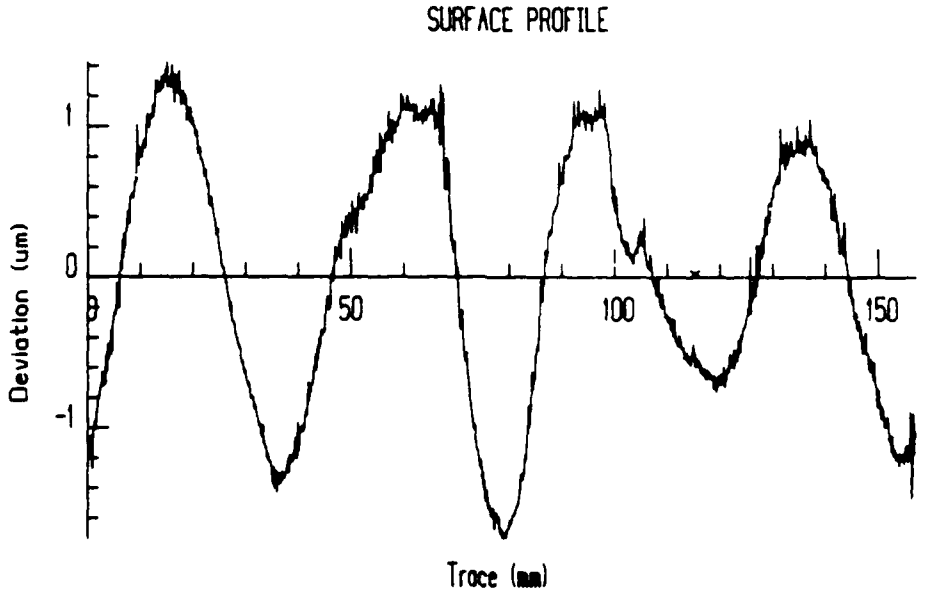

(b) After test

Figure 7. Surface profiles before and after test for 440C stainless steel ring at $R_B 98$.

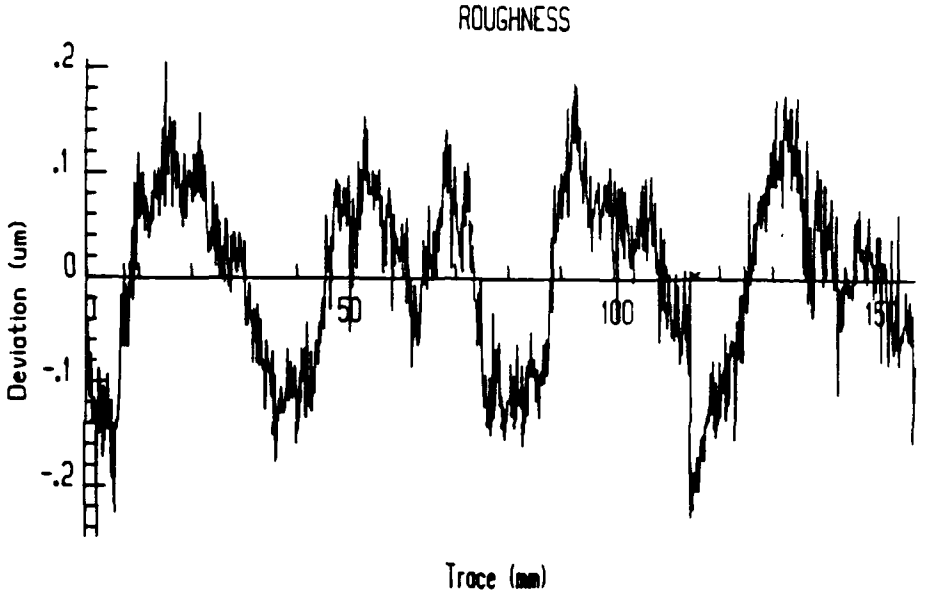

(a) Before test

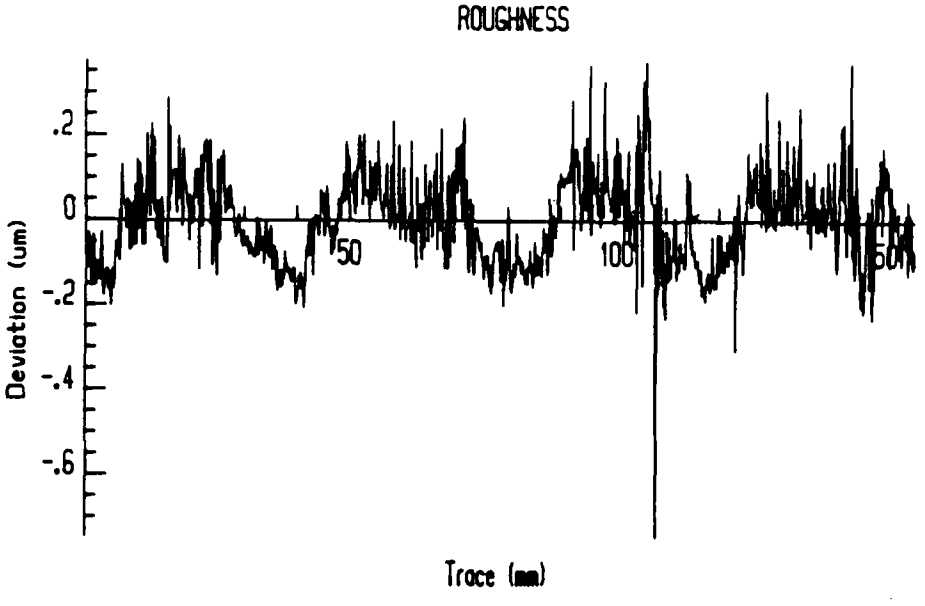

(b) After test

Figure 6 Roughness curves before and after test for 440C stainless steel ring at R_C60.

across the ring interface. A fifth contact was beginning to appear between the second and third patches, although it initially showed up on only one probe (Fig. 4a). Later this contact spread radially across the interface and appeared to be joining with the second contact patch. From the surface profiles (figures 4b and 5b) it can be seen that that fifth contact occurred at a shoulder on the ring profile just after the second waviness peak.

Closer examination of the surface profiles in Figures 4b and 5b shows that wear had occurred at the four peaks of the ring surface, resulting in both a decrease in peak height and a roughened surface within the contact patches. The ring surface, which had been polished to a finish of approximately 0.01 μm Ra before the test, ended up with a roughness two to ten times greater within the contact patch areas after one hour of sliding. This increase in roughness near the contact patches is apparent in Figure 6, which shows the short wavelength surface topography for the ring of Figures 4 and 5. To obtain those roughness curves the long wavelength waviness information was numerically subtracted from the profile data in the data analysis program [8].

Results similar to those shown in Figures 4 and 5 were found for 440 C stainless steel rings of several different hardnesses [10]. In all cases, the waviness peaks, which coincided with contact patch locations, were found to increase in height and become roughened due to wear. An additional example of these results is shown in Figure 7, for the case of a 440 C stainless steel at hardness R_B 98. Note how the peaks of the contact profile were worn and became rougher as a result of wear.

The change in surface profile was even more pronounced with beryllium copper test rings, which showed considerably more wear than those made from 440 C stainless steel. This is shown graphically in Figure 8, in which the before-test and post-test profiles of a beryllium copper ring are compared.

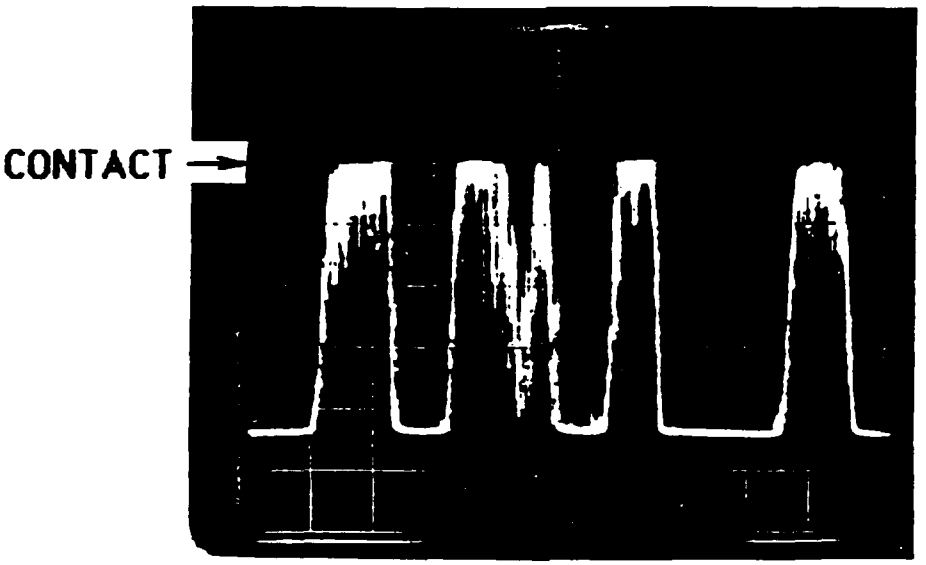

(a) Contact probe output

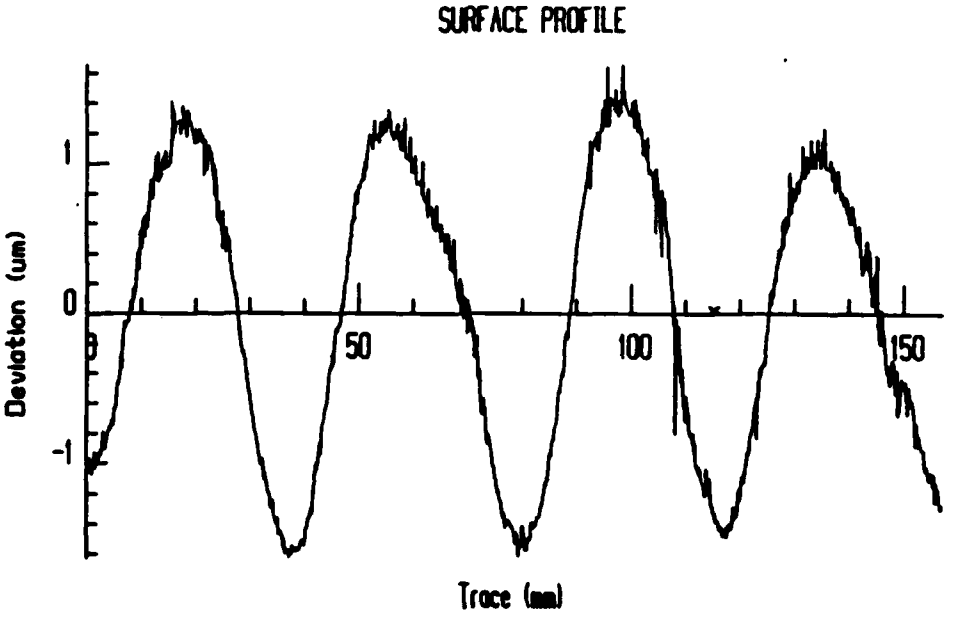

(b) Surface profile after test

Figure 5. Comparison between contact patch output near end of test and surface profile measured after test for 440C stainless steel ring at $R_C 60$.

(a) Contact probe output

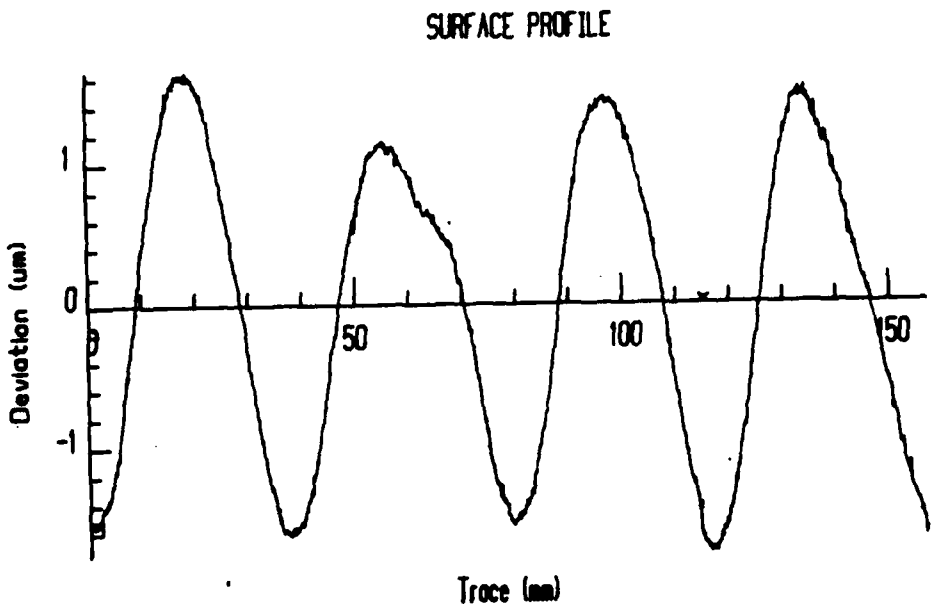

(b) Surface profile before test

Figure 4. Comparison between contact patch output taken immediately after commencement of test and surface profile measured before test for 440C stainless steel ring at P_C60.

440 C stainless steel ring (Rockwell hardness R_C40). The photo was taken after about 15 minutes of testing at 125.7 rad/s. Three distinct contact patches are seen, with some evidence of a fourth forming (at about 40° from starting point). Soon after the photo was taken the seal was disassembled and the surface profile of the metallic ring was measured. As part of the data analysis, any tilt of the ring was subtracted by doing a Fourier analysis of the data and subtracting the first harmonic. The resulting profile is shown in Figure 3b, with the short wavelength surface roughness subtracted.

Comparison between the surface profile and the contact probe photo shows that the locations of these peaks correspond with those measured contact patches. The highest of the peaks, located at about 140°, appears to be at the end of the broadest contact patch, while the smallest peak is at about the same location as the small patch just coming into contact in Figure 3a.

Figures 4 and 5 show a comparison between the surface profiles, including microroughness, and the contact patch locations measured both before and after tests for 440 C stainless steel with Rockwell hardness R_C60. The ring was run dry against carbon graphite for one hour at 125.7 rad/s. Again, close agreement between the two sets of results supports the hypothesis that the contact patch locations coincide with the peaks of the metallic ring's surface profile. For that stainless steel ring there were initially four distinct contact patches within the 157 mm ring circumference (Fig. 4a). All four of the patches were indicated by both probe wires, the one near the O.D. of the contact interface and the other near the I.D. This showed that those patches extended radially

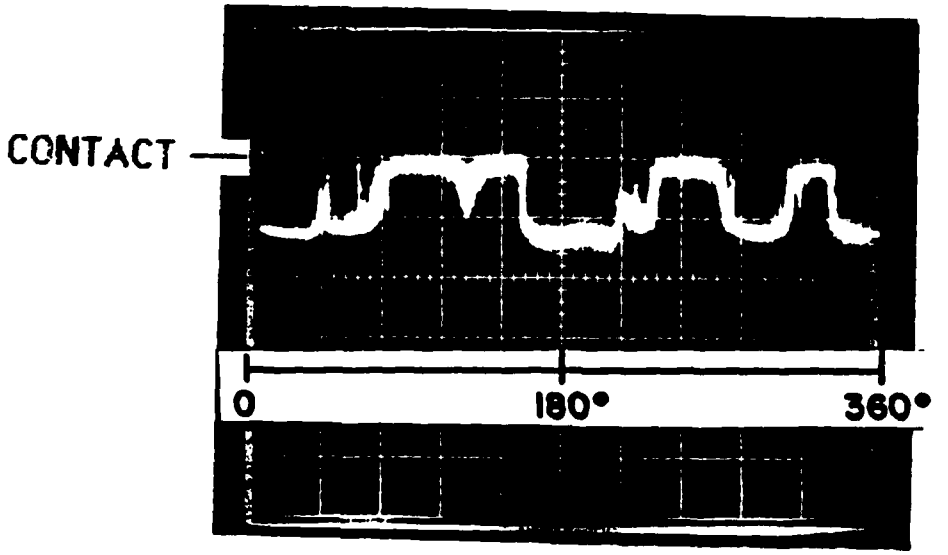

FIGURE 3a Contact probe output after 16 minutes of dry test of rotating 440C stainless steel ring vs. stationary carbon graphite ring at 125.7 rad/sec.

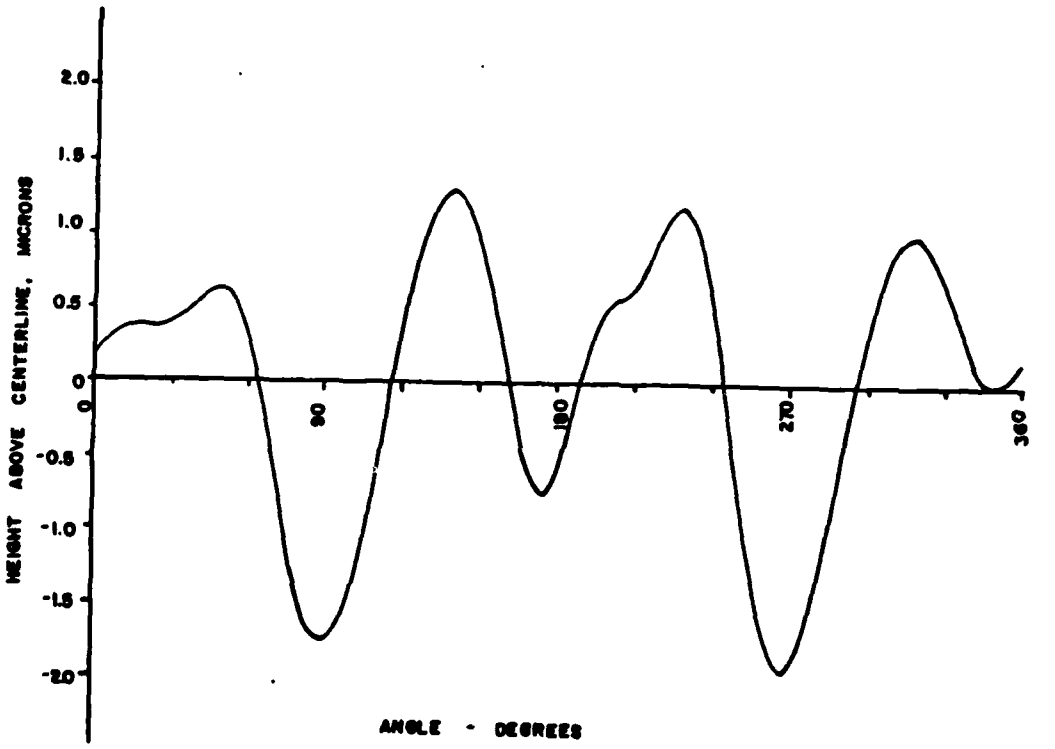

FIGURE 3b. Surface profile of metallic ring after test of Figure 3a.

Figure 3 Comparison between contact probe output and surface profile after test.

cooler contact patches at lower speeds than at higher velocity. The same tendency was noted with 52100 bearing steel mating rings. These results are similar to those found earlier in dry tests of those materials [5].

One result of the liquid lubricated tests that differed from those of the dry tests was a slight tendency of the friction coefficient to be lower at higher velocities, particularly with the 440 C mating rings. The average friction coefficient was 0.15 at 62.8 rad/s, decreasing to 0.13 at 188.5 rad/s. This could be an indication of more effective hydrodynamic lubrication at higher velocities. Another difference between the wet and dry tests was the more unstable nature of the contact patches in the wet cases. As noted above, there were more sudden changes in patch size in the liquid lubricated tests than had been observed in dry cases.

Because of the similarity between these results for liquid lubricated seals and those obtained earlier for dry operation [5], and owing to the additional complexities involved in testing liquid lubricated seals, the rest of the tests in this paper were run in a dry condition.

Relationship Between Surface Profile and Contact Patch Location

When the first measurements of contact patch sizes and locations were made [5], it was hypothesized, but not proven, that the contacts were located at waviness peaks on the contact surface of the metallic ring. Subsequent development of a profilometry data acquisition system in our laboratory [8] has enabled comparison between ring surface profiles before and after testing and the contact probe measurements during operation.

A typical contact probe output trace is shown in Figure 3a. The trace is from a dry test of a carbon graphite stationary ring in contact with a

patches, comprising a total of about 25% of the ring circumference. The temperature in the patches was 85-90°C, according to the dynamic thermocouple output. Later, after about 3 minutes of testing the patches had grown and merged into three large patches, making up nearly 75% of the circumference and having temperatures ranging from 55-60°C (Fig. 2b). Still later, after 7 minutes of testing, there was a shrinkage of the patches that seemed to be accompanied by (or related to) leakage of fluid from the seal. The patches then gradually grew until after about 15 minutes there were again three large contacts similar in size to those in Figure 2b.

At higher speeds there tended to be smaller contact patches, as was the case with dry operation [5]. Tests of beryllium copper rings rotating at 125.7 and 188.5 rad/s showed that the patch sizes generally had settled to a steady size after about 20 minutes of operation. The total patch length was shortest for the 188.5 rad/s test (≈35% of the ring circumference) and was larger (about 50%) for the 125.7 rad/s tests. As was shown in Figure 2b, the contact patches covered a total of about 75% of the ring circumference in the 62.8 rad/s tests. The surface temperature within the patches was found to be higher for shorter patch lengths in these liquid lubricated tests (up to about 150°C for the 188.5 rad/s tests). These temperatures were somewhat lower than those measured in dry tests under the same conditions [5], although the friction coefficient was nearly the same as that measured in the dry tests ($f = 0.15$). An analysis of the surface temperatures indicated that the major reason for the lower temperatures was transfer of heat to the sealed fluid at the inside of the rotating seal ring [10].

Tests with 440 C stainless steel mating rings showed the same trend as that observed in the beryllium copper tests. There were fewer, larger, and

FIGURES 2. Contact probe output during test at 62.8 rad/sec of rotating beryllium copper ring vs. stationary carbon graphite ring with pressurized water as sealed fluid.

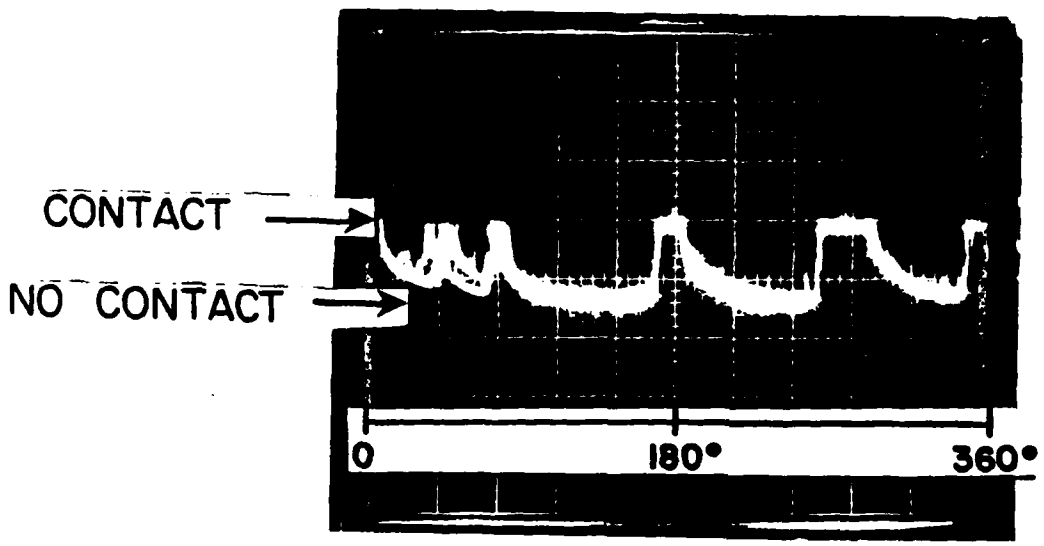

FIGURE 2a. Immediately after commencement of test

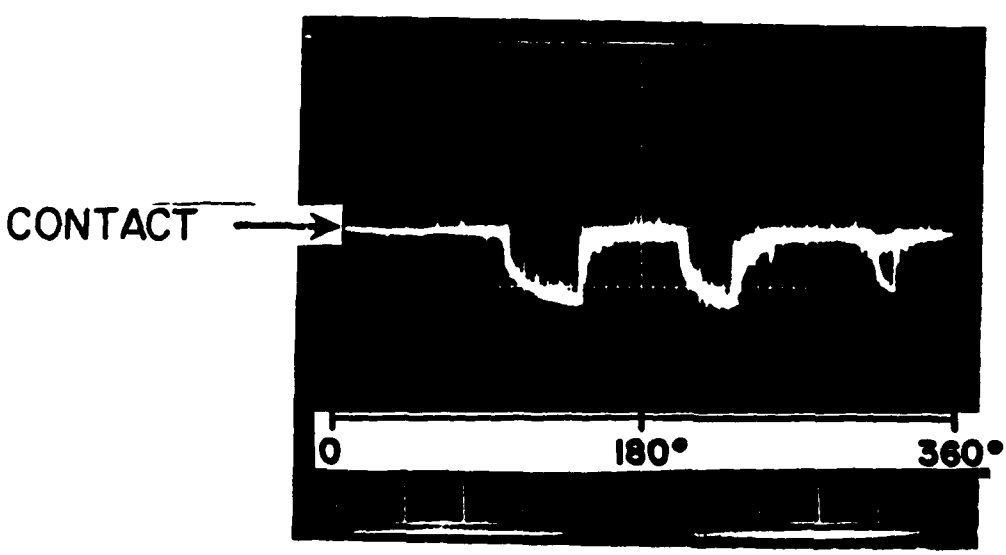

FIGURE 2b. After 3 minutes.

After the test, the metallic ring was again ultrasonically cleaned before weighing (to determine the amount of wear that had occurred) and measuring the surface profile. The wear particles on the carbon graphite ring were removed using compressed air and tissue paper before weighing of that ring.

For the liquid lubricated seal tests, the same procedure described for the dry tests was followed, except that pressurized water was introduced as a sealed fluid at the interior of the seal and wear was not determined. As was the case in earlier tests with liquid lubricated seals [5], there was a tendency for the contact probe signal to be shorted through the thin film of sealed liquid between the seal faces. Nonetheless, careful test procedures, along with a lower fluid pressure, a larger normal force between the seal faces, and some electronic signal filtering enabled the contact probe and dynamic thermocouple to give clear indications in most cases. Water pressures as low as 3500 Pa were used in some tests.

RESULTS AND DISCUSSION

Liquid Lubricated Tests

Many of the results of the liquid lubricated tests were similar to those described earlier [5] for dry tests. A typical set of results is shown in Figure 2 for the case of carbon graphite stationary ring and beryllium copper rotating ring. In Figure 2a is shown a photo of the contact probe output at the beginning of a test at 62.8 rad/s angular velocity. Despite lapping of the rings prior to the test there is evidence of five distinct contact

Experimental Procedures

Each of the metallic rings used in the test program was carefully lapped and polished prior to testing. Once polishing was completed, the ring was ultrasonically cleaned before weighing on an analytical balance. The carbon rings were also lightly lapped and cleaned before being weighed.

Prior to testing the surface profile of each metallic ring was obtained using the profilometer system. The ring was accurately centered on the air bearing rotary table and mechanically levelled to within $\pm 4\mu m$ in most cases. About 45,000 samples of profile data were then obtained around the ring circumference at the center of the contact path.

Following completion of the profile data acquisition process, testing of the specimen could be performed in a dry condition, that is, in room temperature air with no sealed liquid, or in a liquid lubricated condition with sealed water. The test duration for all dry tests was set at 1 hour. Before the start of the test, the rotating metallic ring was lowered onto the carbon mating ring and contact was maintained by applying a constant normal force of approximately 92 N. The contact probe/thermocouple was set in the probe mode and a 5 volt D.C. signal was applied to the rotating ring via the carbon electrical brush placed at its outer diameter. The 5 volt pulses arising from intimate contact between the rotating ring and the probe wire were monitored using an oscilloscope, and photographs were taken of the oscilloscope output at several instants during the course of the test. The contact probe/thermocouple was then switched to the thermocouple mode, in which the 5 volt input signal was turned off, and a small voltage signal was generated at the contact spots where a metal-to-metal junction had been established. This generated emf was also monitored through the oscilloscope. Photos were taken so that contact temperatures could be approximated.

Material	Modulus of Elasticity ($x10^9$ N/m^2)	Thermal Conductivity (W/m-K)	Coefficient of Thermal Expansion ($x10^{-6}$ /C)
440C Stainless Steel (16-18 Cr, .95-1.20 C, 1.0 Mn) (1.0 Si, .04 P, .03 S, .75 Mo)	200	24.2	100.8
52100 Alloy Steel (1.3-1.6 Cr, .98-1.10 C, .25-.45 Mn) (.025 Pmax, .025 Smax, .15-.35 Si)	207	38.05	126.2
Beryllium Copper (97.9 Cu, 1.9 Be, .2 Ni or Co)	131	100.5	167.2
Carbon-Graphite Composite	6.89	11.9	

Table 1. Properties of face seal ring materials.

data, calculated a number of surface roughness parameters, and plotted the surface profile around the ring circumference, along with other relevant topographical information. Further details of the data acquisition and analysis system are given in Appendix A and ref. [8].

Materials

Each of the seals tested in this work consisted of a stationary seal ring made from a commercial carbon graphite material (Pure Carbon grade P658RC) and a rotating metallic ring. All rings were in a configuration similar to that found in the baseline commercial face seal. The sealing surface of each combination had an inside diameter of 5 cm and a width of 2.5 mm.

Three metallic ring materials were used in the tests; 440 C stainless steel (the baseline material), 52100 alloy steel, and beryllium copper. The product of modulus of elasticity times coefficient of thermal expansion differs slightly for these three materials (ranging from $2.0\times10^{7}Nm^{-2}C^{-1}$ for 440 C stainless steel to $2.6\times10^{7}Nm^{-2}C^{-1}$ for 52100 alloy steel). A much more significant difference is found in thermal conductivity which is $24.2Wm^{-1}C^{-1}$ for 440 C stainless steel, $38Wm^{-1}C^{-1}$ for 52100 alloy steel and $100Wm^{-1}C^{-1}$ for beryllium copper [9]. One of the major goals of this work was to study the relationship between the contact patch length and wear resistance, and for that purpose the metallic rings were heat treated to three different hardnesses. One set of rings from each material was hardened to the same Rockwell hardness R_C40. Other rings of 440 C stainless steel were heat treated to achieve a greater hardness, R_C60, while others were left in the annealed condition, where they possessed the hardness R_B98. Details of the heat treatment procedures are given in ref [10]. A summary of the ring material properties is given in Table 1.

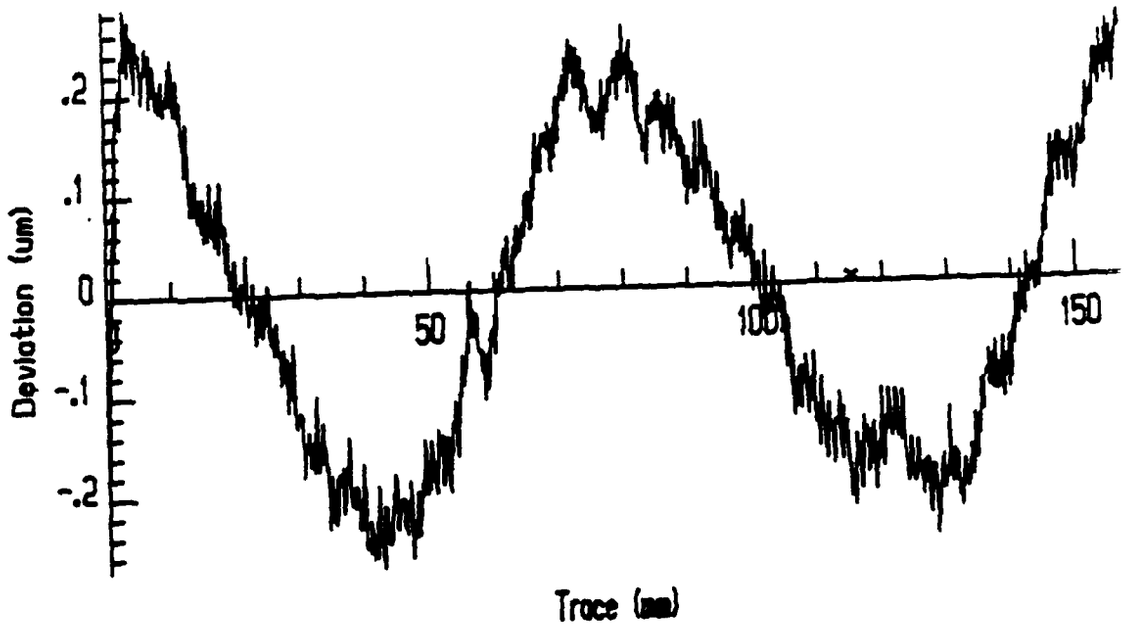

a. Surface profile before test

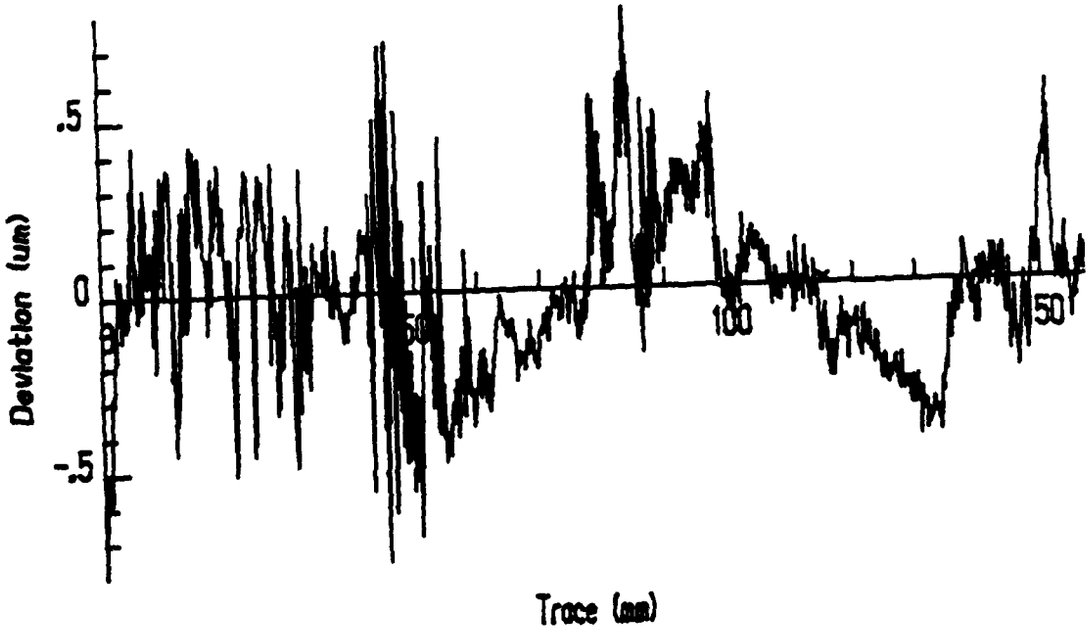

b. Surface profile after test

Figure 8. Comparison between pre- and post-test surface profiles for beryllium copper test ring.

In that case there were initially two contact patches, located at the waviness peaks about 180° apart on the ring surface (Fig. 8a). By the end of the one hour test the contact regions had expanded and joined to cover the entire 157 mm ring circumference. This resulted in about a tenfold increase in roughness over the entire ring surface, and in the virtual disappearance of the initial surface features (Figure 8b). As is evident in Figure 8, considerable wear of the beryllium copper ring surface took place during the one hour test. As was the case with the stainless steel rings, wear occurred only within the patches of contact, but in the beryllium copper case the patches spread over a much larger area, the entire nominal contact area. There was some evidence in tests of 52100 alloy steel rings that the wearing of the contact patches can produce an increase in both surface roughness and waviness [10]. In one test the range of heights of the surface profile increased from approximately ±0.2 μm to about ±2 μm (measured from profile centerline). Although substantial roughening occurred at the waviness peaks, most of the increase in height appeared to result from an increase in wave height [10]. That increase could be caused by some warping introduced by non-uniform wear of the heat treated ring surface.

Effect of Material Properties on Contact Patch Size and Wear

To further examine the influence of ring material properties on the relationship between contact patch geometry and wear, a series of tests was run with five different metallic rings. All rings were tested for one hour in dry sliding against a carbon graphite ring at 125.7 rad/s.

A summary of the test results is given in Table 2. The contact width and wear (weight loss) values given are the mean values of measurement taken from between five and nine tests of each material. Standard deviations of the wear values are given in brackets in the table.

Material	Rockwell Hardness	Microhardness		Total Contact Width, mm		Weight Loss, mg	
		In Wear Track, HV	Outside Wear Track, HV	Beginning	End	Metal	Carbon
440C Stainless Steel	B98	318	254	16	44	0.31 [0.18]	21.30 [8.27]
440C Stainless Steel	C40	450	420	9	35	0.43 [0.44]	19.79 [9.24]
440C Stainless Steel	C60	820	737	6	13	0.56 [1.20]	10.82 [3.11]
52100 Alloy Steel	C40	443	409	25	72	15.92 [3.31]	25.92 [11.58]
Beryllium Copper	C40	411	398	60	157	215.35 [39.53]	35.03 [9.95]

Table 2. Summary of the wear test data for the three metallic rings at Rockwell R_B98, R_C40 & R_C60. Note that numbers in brackets are standard deviations.

An overview of the results reveals a general tendency of the contact width to increase towards the end of the test. An increase in contact patch width was also seen with increases in thermal conductivity. This is in agreement with data reported earlier [5]. Most distinctive is the contact patch width for beryllium copper at completion of the test. After one hour of continuous rubbing, the contact width stretched over the whole circumference of the ring in all of the tests with that material. As was mentioned earlier, beryllium copper has the highest thermal conductivity of the three materials tested, while 440 C stainless steel has the lowest.

It can also be seen from Table 2 that, for the 440 C stainless steel material, the total contact width decreased as the hardness increased from Rockwell $_{B}98$ to Rockwell $_{C}60$. This supports the earlier prediction [5] concerning the formation of smaller, hotter contact patches at higher hardness levels. This is not surprising since it is well known that the contact area required to support a given load is inversely proportional to the hardness of the material. This also means, however, that the differences in contact patch size which were observed for the three materials with the same hardness but different thermal conductivity were not due to a different real area of contact. Instead they are indicative of a concentration, or spreading out, of the real area of contact into different-sized patches.

Table 2 also presents some interesting wear data. Comparing the wear for the three materials of the same hardness (Rockwell $_{C}40$), one sees that increases in wear accompanied increases in contact patch size. The beryllium copper ring had the largest total contact width and experienced considerably more wear than the other, less conductive, materials. Even though all three materials had the same hardness, the wear data clearly indicate that the wear resistance of the beryllium copper ring was much lower than either of the other two materials.

Microhardness measurements in the worn region of each ring showed that each material experienced work hardening in the contact zone, so softening due to frictional heating did not affect wear in these tests.

The wear data also indicate that, in addition to having by far the highest wear, the beryllium copper ring also caused the most wear of the carbon counterface. Thus, from a wear point of view, beryllium copper, the most highly conductive material, would be a poor choice for a face seal application requiring good durability. This result is important since earlier work [4] had concluded that materials which have relatively high thermal conductivity would be less likely to encounter thermocracking and might, therefore, be good candidates for face seals. The large contact patch sizes noted with beryllium copper would indeed lead to reduced near surface stresses with that material, thus making thermocracks less likely. However, those large contact lengths result from the combined effects of beryllium copper's high thermal conductivity and its low resistance to wear, and low wear resistance is undesirable for seal face materials. The mechanisms responsible for beryllium copper's high wear rate could not be ascertained in this series of tests.

Tests of 440 C stainless steel rings at three different hardnesses showed similar patterns of wear, which was concentrated at the contact patch locations. There was a definite tendency toward decreased carbon ring wear in tests against harder stainless steel rings. There was also a slight, and unexpected, increase in metallic ring wear with increases in hardness, but the variability in the wear data, as evidenced by the standard deviation, makes that result somewhat inconclusive. Further tests are being run to confirm that relationship between metallic ring hardness and wear. If later results show a similar increase in metallic ring wear with hardness, it could be because of the more severe temperatures and thermal stresses near the

smaller contact patches associated with the higher hardness materials. Nonetheless, each of the 440 C stainless steel rings, regardless of hardness, showed much less wear than that which occurred with either of the other metallic materials used in this study. This is indicative of better wear resistance for the stainless steel material in this application.

CONCLUSIONS

In conclusion, the results of this year's research can be summarized as follows:

1. Contact patches resulting from thermoelastic instability have been observed to follow a similar trend to those obtained in the previous study [5]. Namely, under both dry and liquid lubricated conditions, the patches tended to remain stationary on the rotating metallic ring, although they were more transitory in nature in the liquid lubricated case. Contact patch sizes tended to be larger and at a lower temperature for beryllium copper ring than those found with 440C stainless steel or 52100 alloy steel rings. Based on the results of the tests, it appears that those ring materials with higher thermal conductivity and lower wear resistance were more conducive to the formation of larger and cooler contact patches (or less prone to thermoelastic instabilities). These phenomena stemmed from a combination of heat conduction and wear, which led to the enlargement of the contact patches. It was observed that decreasing the rotational velocity also resulted in larger contact patches and lower contact temperatures.

2. Surface geometry analysis using the profilometry system has shown that the contact patch locations coincide with

peaks of the surface profile waves. Wear was also found to have occurred at the peaks of the profile, as reflected by the worn surfaces of the peaks and an increase in surface roughness in those regions.

3. Results of the wear tests for three metallic rings at Rockwell$_C$40 show that contact patch size and weight loss of the rings increase with higher thermal conductivity. Beryllium copper, having the highest value of thermal conductivity, had the largest contact width due to the higher rate of heat conduction away from the contact spots and the lower wear resistance of the material. It also experienced the most weight loss, though its hardness was equivalent to the other metallic rings.

   For 440C stainless steel rings at Rockwell R_B98, R_C40 and R_C60, the wear test data showed that total contact width at both the beginning and end of the test decreased as hardness increased from R_B98 to R_C60. Wear of the metallic ring was only very slightly affected by the change in hardness.

4. Based upon the results from this study as well as earlier ones [5], material parameters such as thermal conductivity and wear resistance merit careful consideration when analyzing contact conditions in mechanical face seals. Increasing the thermal conductivity of a material would increase the contact area, thus ensuring maximum uniform contact of the faces and less chance of thermocracking. However, the increase in contact area may be accompanied by undesirable high wear rates, and hence, a decrease in the

operating life of a face seal. On the other hand, comparing the wear data for 440 C stainless steel at R_B98, R_C40 and R_C60 indicates that wear was not affected considerably by increasing the hardness of the material.

REFERENCES

1. Burton, R.A., Nerlikar, V. and Kilaparti, S.R., "Thermoelastic instability in a seal-like configuration", Wear , 24 (1973), 177-188

2. Lebeck, A.O., "Theory of thermoelastic instability of rotating rings in sliding contact with wear", ASME J. Lub. Tech., 98, 277-285

3. Banerjee, B.N. and Burton, R.A., "Experimental studies on thermoelastic effect in hydrodynamically lubricated face seals", ASME J. Lub. Tech., 101 (1979), 275-282

4. Kennedy, F.E. and Karpe, S.L., "Thermocracking of a mechanical face seal," Wear, 79 (1982), 21-36

5. Kennedy, F.E. and Grim, J.N., "Observation of contact conditions in mechanical face seals," ASLE Trans., 27 (1984), 122-128

6. Kennedy, F.E., Grim, J.N. and Chuah, C.K., "An experimental/numerical study of contact phenomena in face seals," to be published in Proc. 10th Leeds-Lyon Symposium on Tribology, Butterworths, London, 1984

7. Dow, T.A. and Burton, R.A., "Thermoelastic instability of sliding contact including the effects of wear," ASME J. Lubr. Technol., 95 (1973), 71-75

8. Brote, F.O.W., "Design of a data acquisition and data analysis system for surface profilometry," Master of Engineering Thesis, Dartmouth College, June 1984

9. Metals Handbook, American Society of Metals, Metals Park, Ohio, 8th Edition, 1961

10. Chuah, C.K., "Contact phenomena and wear of mechanical face seals," Master of Engineering Thesis, Dartmouth College, November 1984

APPENDIX

Description of Surface Profilometry System

Study of the location of contact patches on surfaces and wear within the patches necessitated the characterization of the seal ring surfaces before and after test runs. This task was handled by profilometry techniques. The system was built around a linear profilometer (Bendix Proficorder) which was designed to perform surface topographical studies of straignt traces over flat surfaces. In order to accomplish profile analysis around a circular trace on a flat seal ring a high accuracy air bearing rotary table (Alpha-Round) was purchased. The motor driven rotary table was used to rotate the ring beneath the stationary stylus of the profilometer.

The profilometer was designed to produce a chart record of the surface profile and a measure of the surface's average roughness (Ra) value. More information about the surface profile was desired than the profilometer could provide. This was accomplished by designing a computer-based system for the acquisition and analysis of the surface profile data. Complete details of that system are given in ref. [8] and a brief description will be presented here.

The system consists of a microcomputer consisting of a personal computer (IBM PC-XT) with peripheral equipment, and mainframe computers (DEC VAX 11-785 and Honeywell DPS 8). The personal computer is equipped with an analog/digital input/output board (Data Translation DT 2805) that is programmable and has a 12 bit analog/digital converter that can sample analog surface profile data (from the profilometer) at rates of up to 13.7 kHz. A direct memory access (DMA) controller enables the board to write the digitized data directly into random access memory on the PC.

The data are sent, via a high speed link, to one mainframe computer (VAX 11-785) for data analysis and another (Honeywell) for graphical output of the results.

When a profile is to be taken of a surface, the specimen is mounted under the stylus, the tracer is set to run with the center line of the profile in the middle of the record, and the range of surface heights is set on the amplifier. The profilometer produces an analog output directly proportional to the stylus motion.

The analog signal is connected to an Analog to Digital Converter, ADC, that transforms the signal from analog to digital form. To gain sufficient resolution, a 12 bit converter is utilized. This means that the range will be divided into 4096 quantization levels, or a relative error less than 0.025%. The Data Translation board contains besides the ADC a Direct Memory Access (DMA) Controller and a parallel port for communication with a computer. Circuitry to set range, offset, and gain for the input signal to the ADC is also provided.

Once the signal has been digitized by the analog to digital converter the 12 bit word is forwarded to the PC. The DMA controller has to be programmed to perform the task of reading the data from the ADC and sending it to the parallel output port of the Data Translation board. The PC will initially store the data in random access memory (RAM). Once all the desired conversions are done the PC will store the data in non-volatile memory, a Winchester disc in this case. The maximum number of datapoints that can be gathered is determined by how much random access memory there is available for storage of datapoints.

The sampling rate has to be specified for each case, depending on the character of the surface, the relative speed between the stylus and the surface and the information that is desired from the analysis. For tests where short wavelength information (roughness) is of interest a high sampling rate and a low relative speed are desired. If only the waviness is of interest a lower sampling rate at a higher relative speed will do. A sampling rate up to 13700 Hz can be performed by the ADC but the user can only set it to a maximum of 1000 Hz since there is no interest in higher sampling rates. The sampling rate was measured to be accurate to within ± .01%.

To initialize the PC for the task of data acquisition the user runs the program for data gathering and data storage which is named Profilec. Profilec is written in Microsoft Basic and uses the PC-DOS operating system. A flowchart for the Profilec program is included in Figure A1. The user is asked to answer questions to get the information that is necessary for later analysis of the data. The user sets the sampling rate, number of samples to be taken, and tells the system when to start the data acquisition process. When all the data have been stored on the Winchester disc the initial part of surface analysis has been completed. If the user wants to store the data file on a diskette he needs only copy the file from the Winchester disc to a diskette.

The data file is then transferred to a Digital Equipment Corporation Vax 11-785 mainframe computer for analysis of the data. The reason for doing the analysis on mainframe computer instead of doing it on the PC is the large amount of numerical processing that is required for the analysis of the surface data. To reduce the analysis time a larger mainframe computer is employed. To transfer files between the PC and a mainframe computer the Kiewit computer network is utilized. (Kiewit is Dartmouth's computer center).

A Fortran77 program called Procalc has been written to perform the data analysis. A flowchart of the Procalc program is presented in Figure A2. The program calculates a large number of surface roughness parameters, including average (Ra), RMS, and total (R_t) roughness, skew, kurtosis, and radius of curvature of asperities. The user runs the program and supplies the name of the data file and the name of the output file. The output file contains all the information that is to be passed to the graphics program. The user has the option to have the autocorrelation function and the power spectral density function calculated. There are also options for setting the limits of the trace to be used for the analysis, setting the cutoff between waviness and

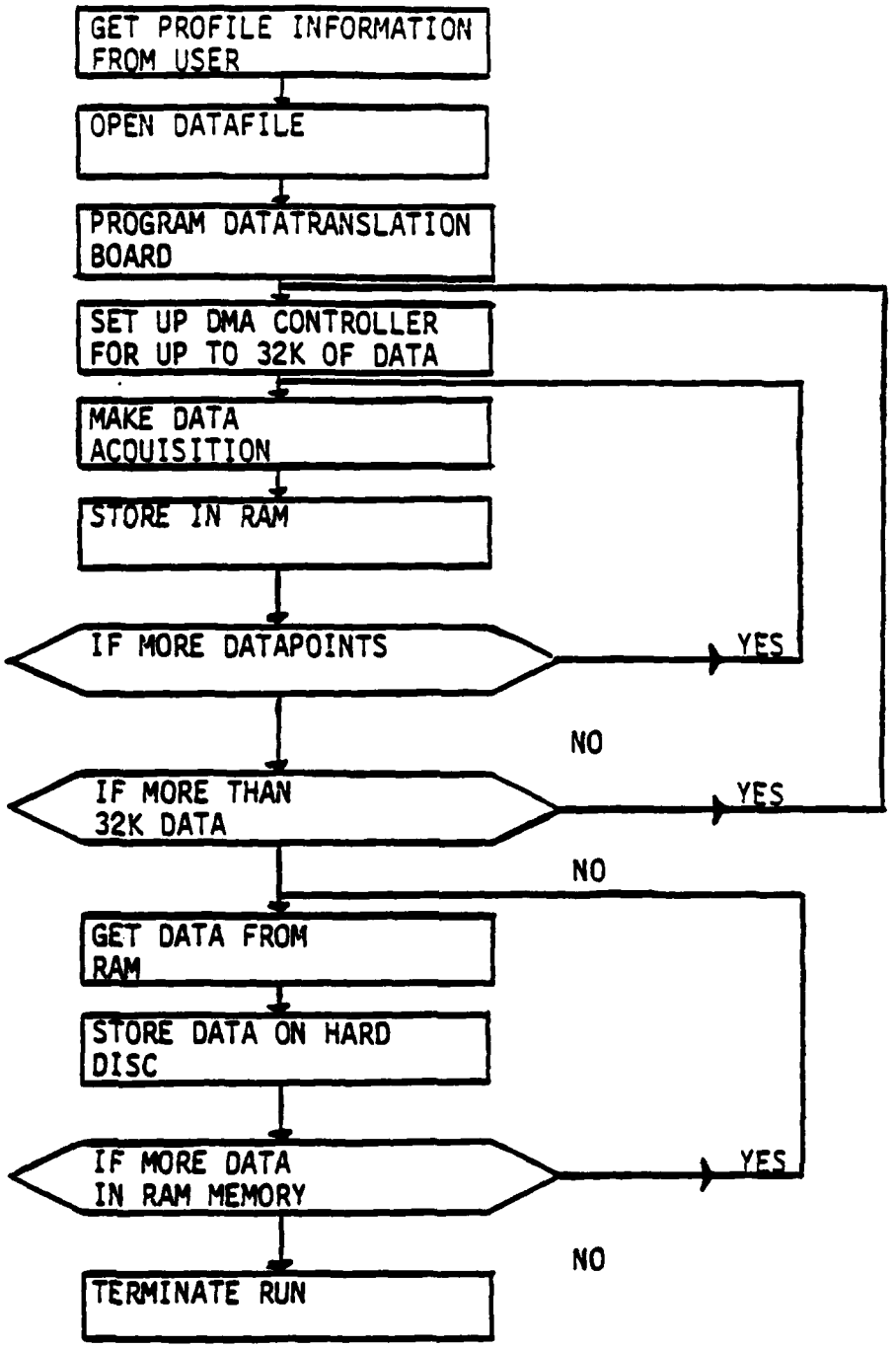

Fig.A1 Flowchart for Profilec

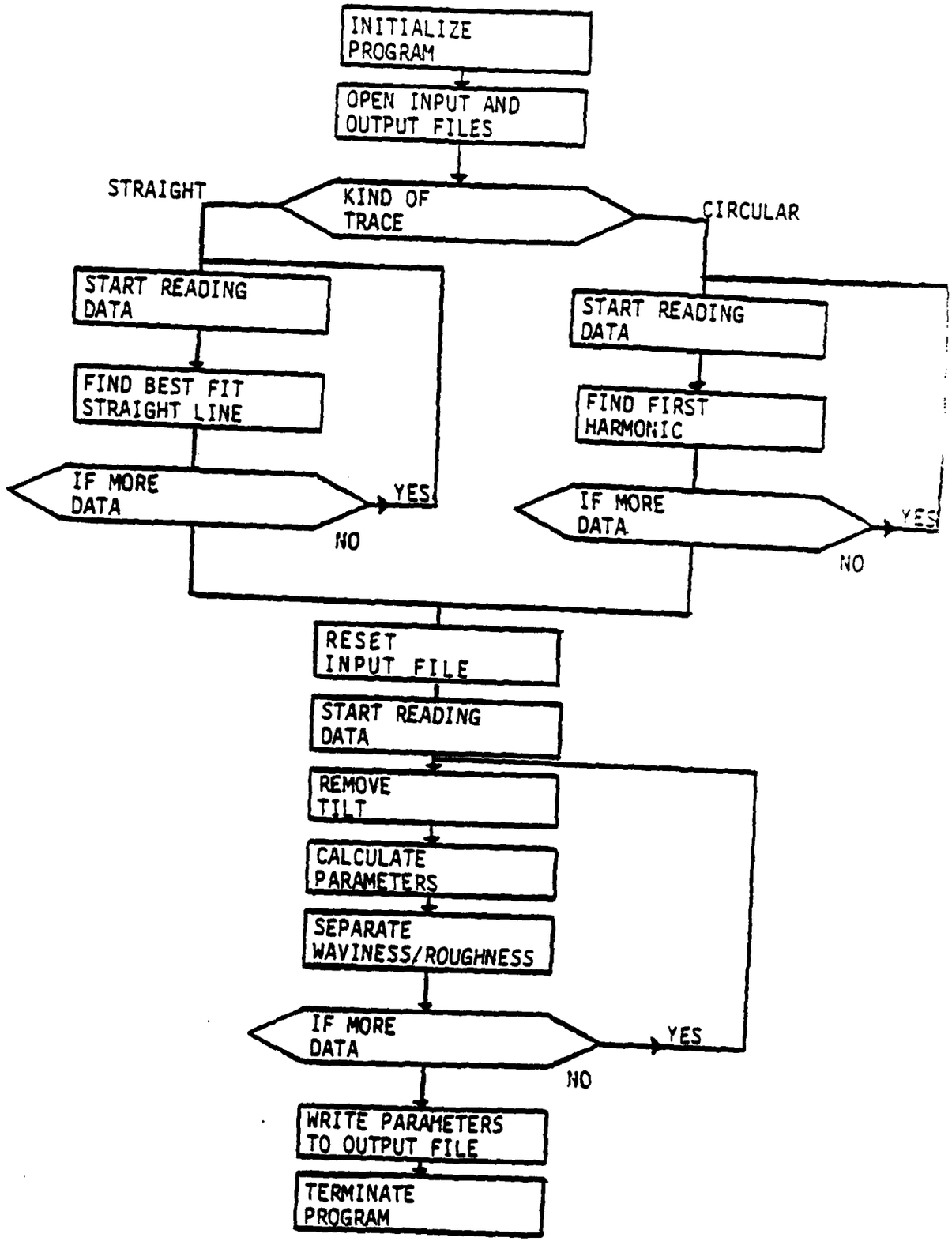

Fig. A2 Flowchart for Procalc

roughness, and if a harmonic analysis or best fit straight line should be utilized to remove the tilt of the sampled profile (a harmonic analysis is used with circular traces, while a straight line fit is employed for straight traces).

In order to take advantage of available computer graphics facilities, the output data from the Procalc program is sent to another mainframe computer (Honeywell DPS 8) for plotting. Again the high speed Kiewit network is used. The data can be plotted in either of two forms. One done on a flat bed plotter (Tektronix 4663) enables a complete record of all surface profile information to be presented on a single sheet. An example of this form of output is presented in Figure A3. That sheet contains seven separate plots of surface topographical information: complete surface profile (corrected for tilt), the long wavelength portion of the profile (waviness), the short wavelength profile information (roughness), a histogram of height distributions, an Abbot (bearing area) curve, and plots of autocorrelation and spectral density functions. Also, included is a listing of the sixteen surface parameters calculated for the profile. Occasionally the user is not interested in all the information presented in the complete record, so another graphical program allows plotting of individual plots on any graphics monitor. Those plots, examples of which are shown in Figures A4 and A5, are chosen by the user from a menu. The surface profile plots in the body of this report were produced by this program.

FIGURE A3 Sample plot of complete surface profile information for straight trace

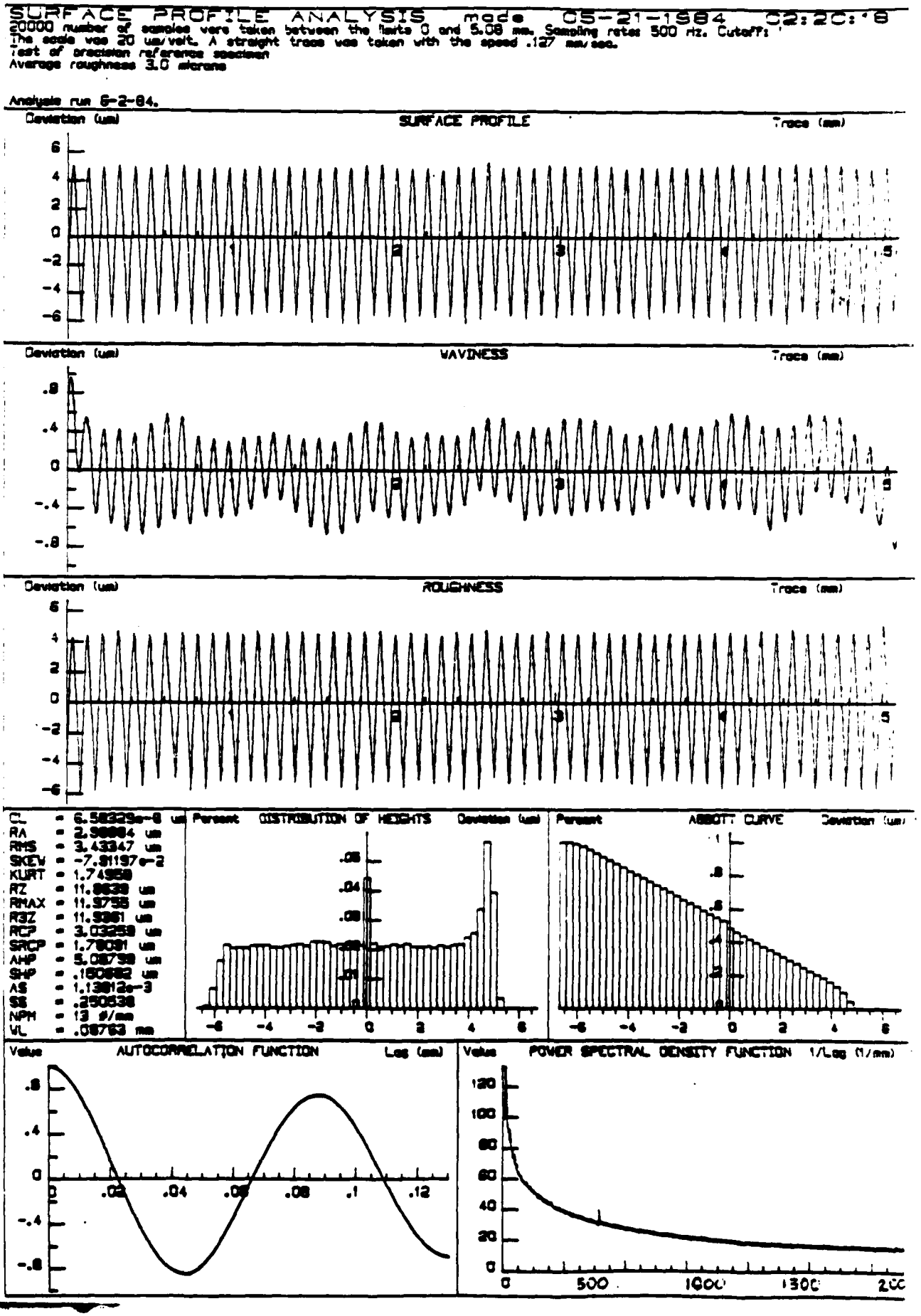

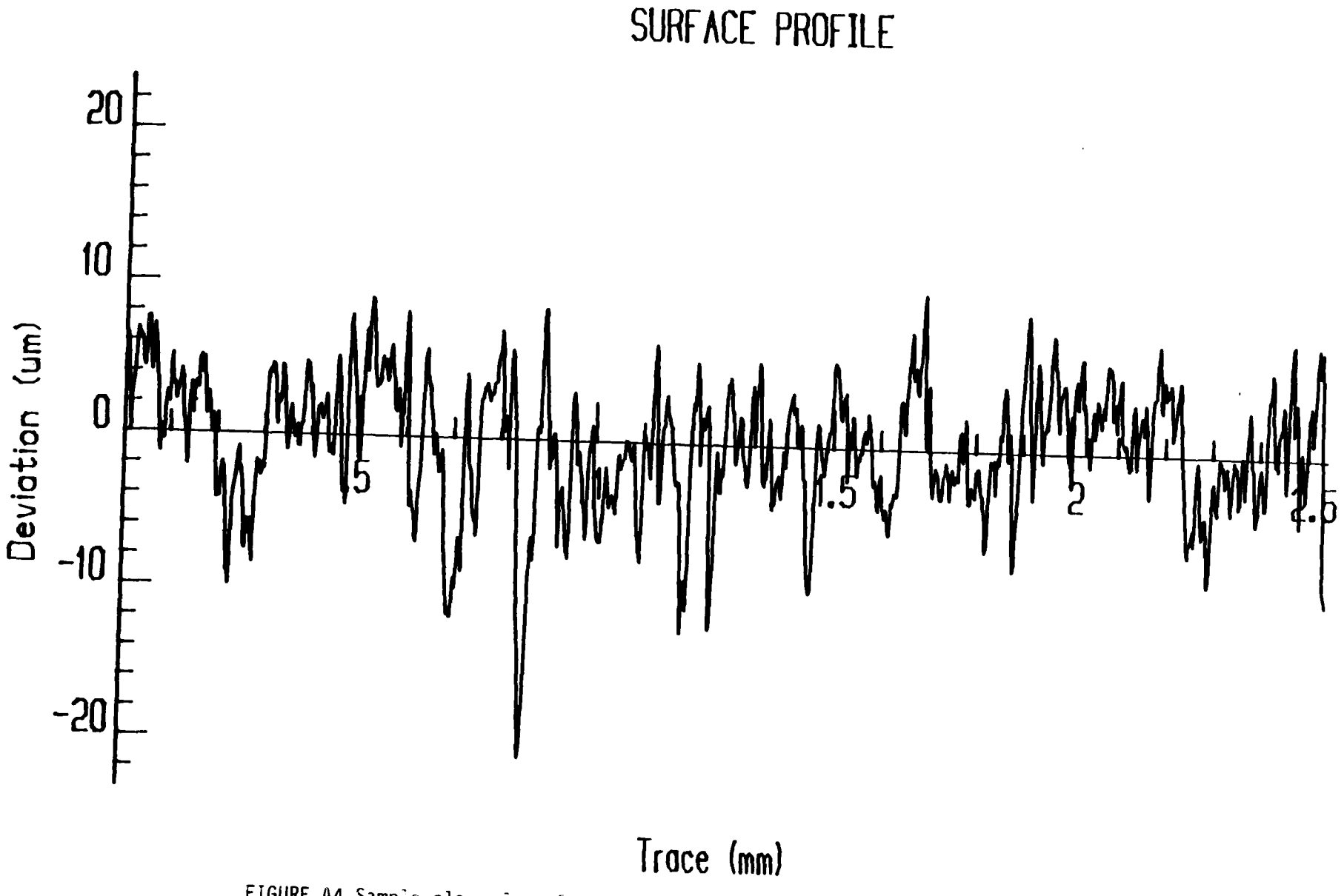

FIGURE A4 Sample plot of surface profile only for straight

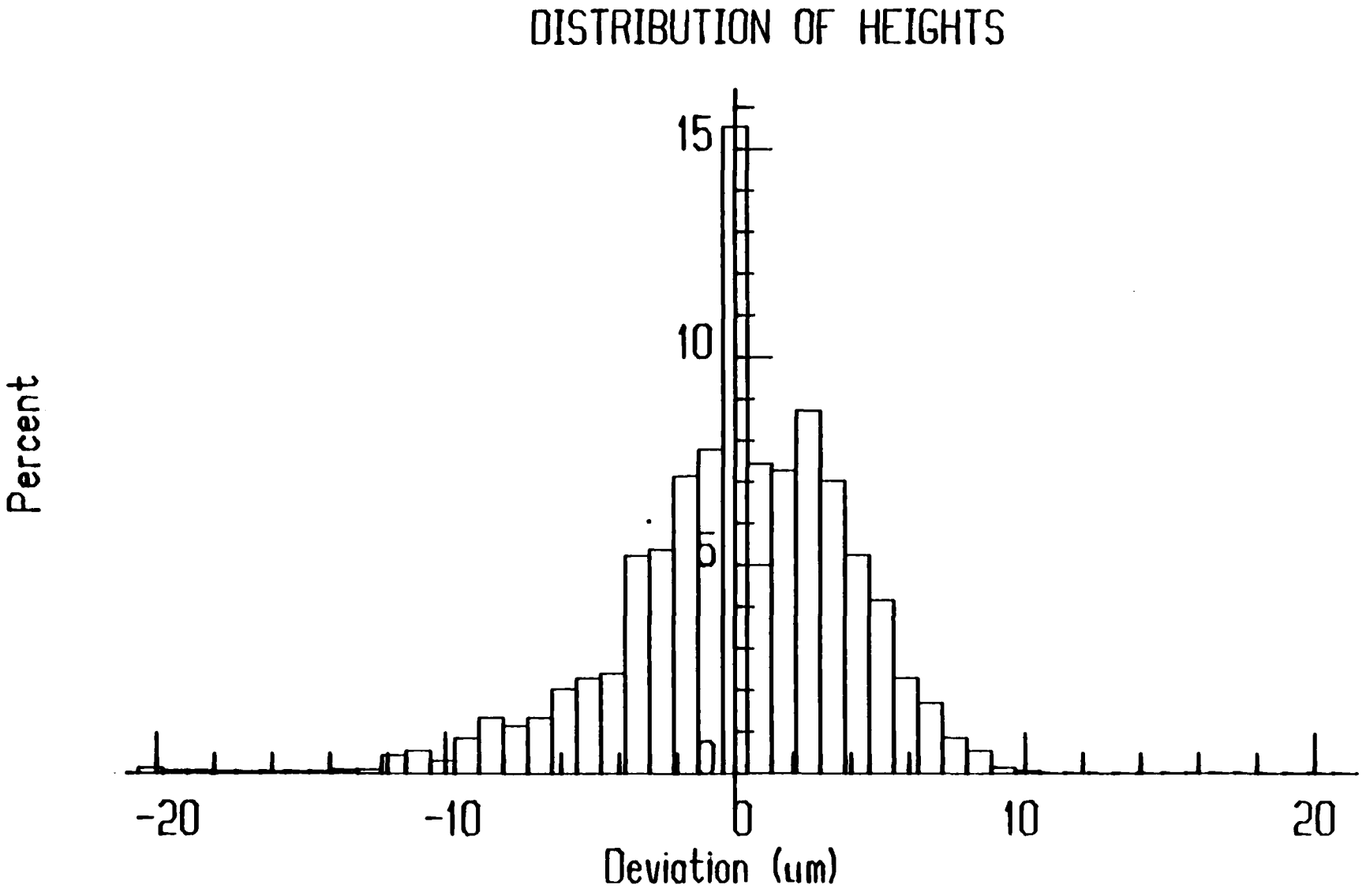

FIGURE A5 Sample plot of height distribution only for straight trace

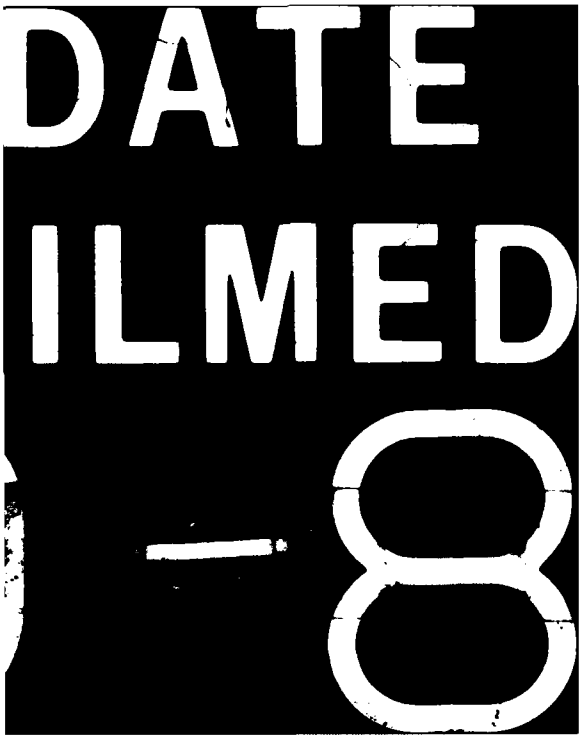
DATE
ILMED
-8